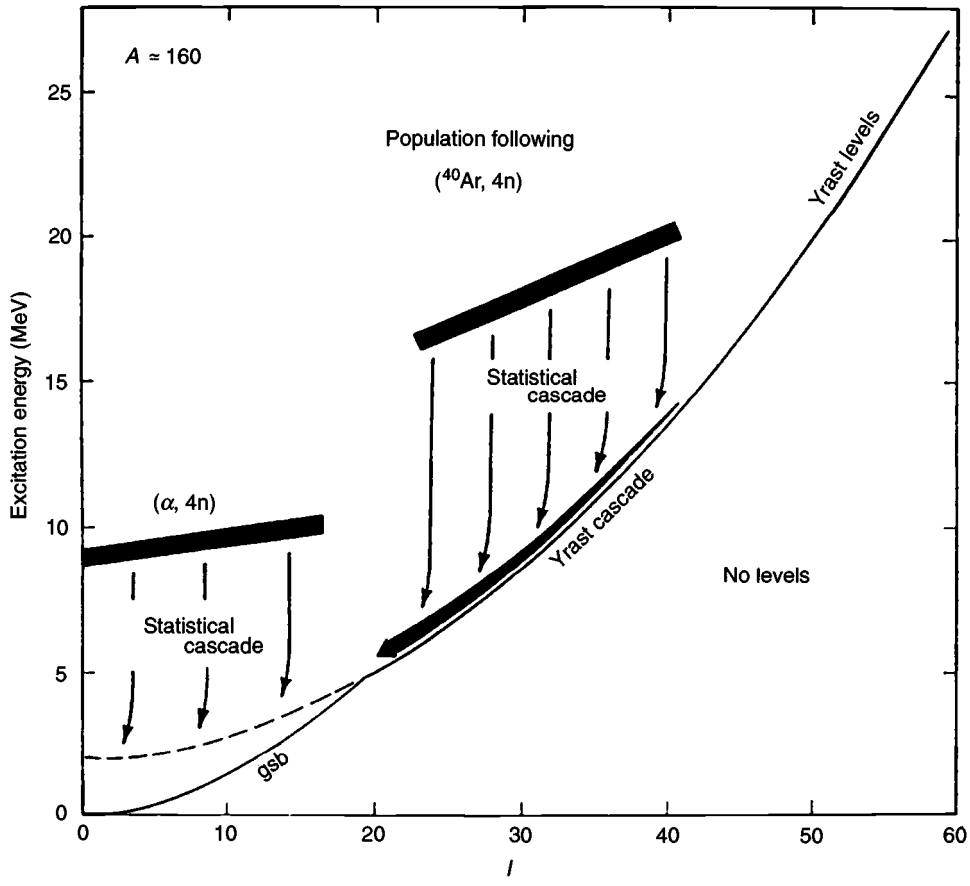

Fig. 11.11. Schematic illustration of which nuclear states are populated in reactions where either ^{40}Ar or an α-particle fuses with a target nucleus to form a compound system with $A \simeq 160$. Such reactions are best suited for the study of the yrast states, i.e. the lowest energy states for each spin I (partly from Stephens and Simon, 1972).

Some additional excitation energy might be carried away by a few so called statistical γ-rays and the yrast region is reached. The additional excitation energy is now carried by the rotational motion. For collective rotation, the compound nucleus will now de-excite mainly through E2 transitions, $(I+2) \rightarrow I$, along the yrast line. A situation like in fig. 11.10 will then lead to E2 energies that are larger for spins $I = 8$–10 than for spins $I = 14$–16.

In fig. 11.11 is also illustrated that the real high spin states can only be reached in so called heavy-ion collisions where both the projectile and the target are heavy nuclei. If an α-particle is used as projectile, only lower spin states can be reached (see problem 11.4).

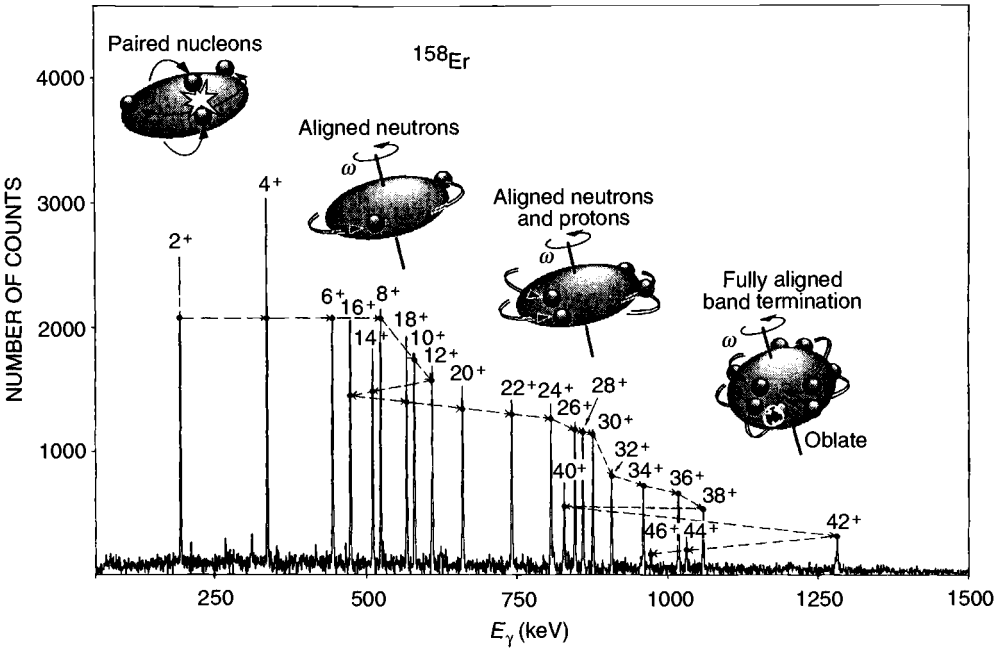

Fig. 11.12. Observed γ-ray energies of ^{158}Er formed in a reaction like the one illustrated in fig. 11.11. For $I \approx 14$ two $i_{13/2}$ neutrons become aligned resulting in a backbend while a second irregularity caused by the alignment of two $h_{11/2}$ protons is seen for $I \approx 32$. The features for $I \geq 38$ with the final band termination for $I = 46$ are discussed in chapter 12.

As seen in fig. 11.12, the experimentally observed E2 energies of ^{158}Er in the range $I = 12$–18 show the properties expected from the simple model of fig. 11.10. Of course, one must expect that the ground band and the decoupled band interact in the crossing region giving rise to a smoother transition between the two bands than shown in fig. 11.10. This is in agreement with the experimental spectrum of ^{158}Er. We must also remember that the model we have described is very much idealised. Still it seems to contain the main features of the physical effect.

The feature that the yrast E2 transition energies suddenly become smaller with increasing spin is generally referred to as back-bending (see fig. 11.12). When investigating such spectra, the yrast energies are often plotted in a somewhat different way. An effective moment of inertia as a function of the spin I can be obtained as

$$\frac{2\mathcal{J}}{\hbar^2} = \left(\frac{\mathrm{d}E}{\mathrm{d}I(I+1)}\right)^{-1} \simeq \left(\frac{E_I - E_{I-2}}{4I-2}\right)^{-1}$$

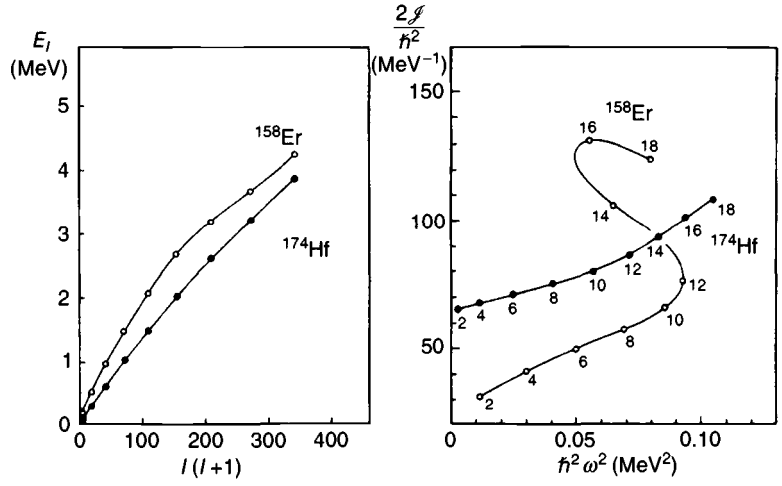

Fig. 11.13. Yrast energies in the $I = 0$–18 range of ^{158}Er and ^{174}Hf plotted versus $I(I+1)$ and corresponding back-bending plots with the moment of inertia $\mathcal{J}$ versus the squared rotational frequency, ω^2 (from R.M. Lieder and H. Ryde, *Adv. in Nucl. Phys.*, eds. M. Baranger and E. Vogt (Plenum Publ. Corp., New York) vol. 10 (1978) p. 1).

The canonical relation between the spin I and the rotational frequency ω is

$$\omega = \frac{\partial H}{\partial I}$$

Thus, in the quantum mechanical case it is natural to define

$$\hbar\omega = \frac{E_I - E_{I-2}}{[I(I+1)]^{1/2} - [(I-2)(I-1)]^{1/2}}$$

which formula is often simplified to

$$\hbar\omega = \frac{E_I - E_{I-2}}{2}$$

i.e., twice the rotational frequency is equal to the E2 transition energy.

A standard back-bending plot shows the moment of inertia $2\mathcal{J}/\hbar^2$ as a function of the squared rotational frequency. This is illustrated for ^{158}Er and ^{174}Hf in fig. 11.13. Note that while the yrast lines, E versus $I(I+1)$, look rather similar, the differences are blown up in the $\mathcal{J}$ versus ω^2 plot. Thus, ^{158}Er shows back-bending while ^{174}Hf does not.

The yrast states of ^{160}Yb and ^{164}Hf are shown in an alternative back-bending plot, I (or rather the component I_x) versus ω, in fig. 11.14. In the spin region $I = 10$–14, two $i_{13/2}$ neutrons get aligned for each nucleus. The second irregularity (up-bend) seen for ^{160}Yb at $I \approx 28$ and for ^{158}Er at